IκBε-Deficient Mice: Reduction of One T Cell Precursor Subspecies and Enhanced Ig Isotype Switching and Cytokine Synthesis[1]

Sylvie Mémet,[2]* Dhafer Laouini,[†] Jean-Charles Epinat,[3]* Simon T. Whiteside,[4]* Bertrand Goudeau,* Dana Philpott,[‡] Samer Kayal,[§] Philippe J. Sansonetti,[‡] Patrick Berche,[§] Jean Kanellopoulos,[†] and Alain Israël*

Three major inhibitors of the NF-κB/Rel family of transcription factors, IκBα, IκBβ, and IκBε, have been described. To examine the in vivo role of the most recently discovered member of the IκB family, IκBε, we generated a null allele of the murine *IκBε* gene by replacement of all coding sequences with *nlslacZ*. Unlike IκBα nullizygous mice, mice lacking IκBε are viable, fertile, and indistinguishable from wild-type animals in appearance and histology. Analysis of β-galactosidase expression pattern revealed that IκBε is mainly expressed in T cells in the thymus, spleen, and lymph nodes. Flow cytometric analysis of immune cell populations from the bone marrow, thymus, spleen, and lymph nodes did not show any specific differences between the wild-type and the mutant mice, with the exception of a reproducible 50% reduction of the $CD44^{-}CD25^{+}$ T cell subspecies. The IκBε-null mice present constitutive up-regulation of IgM and IgG1 Ig isotypes together with a further increased synthesis of these two isotypes after immunization against T cell-dependent or independent Ags. The failure of observable augmentation of constitutive nuclear NF-κB/Rel-binding activity is probably due to compensatory mechanisms involving IκBα and IκBβ, which are up-regulated in several organs. RNase-mapping analysis indicated that IL-1α, IL-1β, IL-1Ra, and IL-6 mRNA levels are constitutively elevated in thioglycolate-elicited IκBε-null macrophages in contrast to GM-CSF, G-CSF, and IFN-γ, which remain undetectable. ***The Journal of Immunology*****, 1999, 163: 5994–6005.**

The NF-κB family of transcription factors controls the expression of a wide array of genes, such as genes encoding cytokines (IL-1α and β, IL-2, IL-6, IL-8, TNF-α, GM-CSF, etc), cytokine receptors, adhesion proteins, immunoregulatory molecules (MHC class I, etc), antiapoptotic and acute-phase response proteins, in addition to viral promoters, like CMV or HIV (1–3), and thus plays a key role in immune and inflammatory processes, as evidenced by recent knockout analyses of NF-κB genes in mice (4–7). NF-κB molecules consist of homo- and heterodimeric combinations of proteins of the same family, which comprises five members in mammals, p50, p52, p65 or RelA, c-Rel, and RelB (1, 2, 6). These proteins share a 300-aa NH_2-terminal Rel homology domain, involved in DNA binding, dimerization, and nuclear localization (8). In contrast to p65, c-Rel, or RelB, which contain a C-terminal transactivation domain, p50 and p52 are synthesized as precursor molecules, p105 and p100, respectively, which are solely cytoplasmic and do not bind DNA. NF-κB/Rel complexes are constitutively active in the nuclei of mature T and B lymphocytes as well as in neurons of certain regions of the brain (8, 9). In the vast majority of cells, however, NF-κB/Rel complexes are sequestered in the cytoplasm by interaction with inhibitory molecules, called IκBs,[5] which mask the NF-κB nuclear localization and DNA binding domains (6, 8, 10). Multiple stimuli, as varied as exposure to proinflammatory cytokines like TNF or IL-1, viral infection, or chemical agents such as phorbol esters, UV irradiation, and phosphatase inhibitors, converge via distinct signaling pathways to activate NF-κB by phosphorylation of IκBs, which leads to IκB ubiquitination and subsequent proteolytic degradation by the proteasome (2). Free NF-κB/Rel complexes then migrate to the nucleus and activate transcription of their target genes.

The IκB family comprises three major members, IκBα, IκBβ, and IκBε, defined by the presence of six ankyrin repeats, a 33-aa motif that mediates protein-protein interactions (10). IκBα and IκBβ were originally purified from cytosolic fractions as NF-κB-associated inhibitory activities (11, 12) and their genes were cloned soon after (13, 14). IκBε was recently identified in yeast two-hybrid screens on the basis of protein-protein interactions with p52 (15), p50 (16), or p65 (17). Despite their extensive structural

*Unité de Biologie Moléculaire de l'Expression Génique, Centre National de la Recherche Scientifique Unité de Recherche Associée 1773, [†]Unité de Biologie Moléculaire du Gène, Institut National de la Santé et de la Recherche Médicale U277, and [‡]Unité de Pathogénie Microbienne Moléculaire, Institut National de la Santé et de la Recherche Médicale U389, Institut Pasteur, Paris, France; and [§]Institut National de la Santé et de la Recherche Médicale U411, Faculté de Médecine Necker, Paris, France

Received for publication June 14, 1999. Accepted for publication September 15, 1999.

The costs of publication of this article were defrayed in part by the payment of page charges. This article must therefore be hereby marked *advertisement* in accordance with 18 U.S.C. Section 1734 solely to indicate this fact.

[1] This work was supported by grants from Institut National de la Santé et de la Recherche Médicale, Agricultural Research Council, Ligue Nationale Française contre le Cancer, Agence Nationale de Recherches sur le SIDA, and European Economic Community.

[2] Address correspondence and reprint requests to Dr. Sylvie Mémet, Unité de Biologie Moléculaire de l'Expression Génique, Institut Pasteur, 25 rue du Dr. Roux, 75724 Paris Cédex 15, France. E-mail address: symemet@pasteur.fr

[3] Current address: Biology Department, Boston University, 5 Cummington St., Boston, MA 02215.

[4] Current address: Hybrigenics SA, Campus Pasteur, 25 rue du Dr Roux, 75724 Paris Cédex 15, France.

[5] Abbreviations used in this paper: IκB, inhibitory protein that dissociates from NF-κB; ALLN, *N*-acetyl-leu-leu-norleucinal; ES, embryonic stem; FDG, fluorescein-di-β-D-galactopyranoside; IL-1Ra, IL-1R antagonist; IRES, internal ribosome entry site; KLH, keyhole limpet hemocyanin; MEF, mouse embryonic fibroblast; X-gal, 5-bromo-4-chloro-3-indolyl β-D-galactopyranoside.

0022-1767/99/$02.00

similarities, IκBα, IκBβ, and IκBε behave differently in response to external stimuli. Generally, IκBα is rapidly degraded and resynthesized, whereas IκBβ and IκBε are degraded with a slower kinetics to gradually reappear (15, 18). Newly synthesized IκBα has been shown to be responsible for postinduction repression of NF-κB activity by entering the nucleus and removing NF-κB/Rel complexes from target promoters (19). The nuclear export sequence of IκBα, which is exposed upon binding to NF-κB, then drives NF-κB/IκBα complexes out of the nucleus (20). Newly synthesized, hypophosphorylated forms of IκBβ interact with the NF-κB/Rel complexes bound on target promoters, without disrupting the DNA-binding interaction, thereby leading to a sustained NF-κB response by protecting the NF-κB molecules from inhibition by nuclear IκBα (21). IκBε is exclusively cytoplasmic and has been found specifically associated with c-Rel, p65 homodimers, or p65/c-Rel heterodimers in cell extracts (15, 16). It is unclear whether different IκB family members have distinct roles or redundant functions in vivo. To address this question, knockout and knockin studies at the *IκBα* locus together with gain of function analysis of IκBα and IκBβ, under the control of T cell-specific promoters, have recently been undertaken (22–26). IκBα knockout mice die by 7 to 8 days after birth and exhibit extensive granulopoiesis, acute runting, and abnormal skin formation (22, 23). Interestingly, the absence of IκBα induces the up-regulation of IκBε (15) and renders mouse embryonic fibroblasts (MEFs) unable to terminate the NF-κB activation after TNF treatment (22, 23). These results confirm the essential role of IκBα in postinduction repression and demonstrate that this function cannot be substituted for by IκBβ or IκBε. Mice containing a knockin of the *IκBβ* coding region at the *IκBα* locus are, on the contrary, totally viable and show no difference in constitutive or induced NF-κB response compared with wild-type mice (24). These data indicate that IκBα and IκBβ share enough biochemical properties to substitute one for another and that their specific in vivo roles arise from their distinct expression patterns.

To gain insight into the physiological role of IκBε, we created IκBε null-mutant mice by targeted *IκBε* gene replacement with *nlslacZ*. Such mice develop normally and do not exhibit morphological defects. Analysis of β-galactosidase activity in these mice reveals that, within the immune system, *IκBε* is expressed mainly in thymocytes. IκBε-deficient animals have normal mature hemopoietic cells, in spite of a 50% reduction in the number of $CD44^{-}CD25^{+}$ precursor T cells. They respond normally to mitogenic stimuli and bacterial challenge, but have an altered basal and Ag-specific Ig production. The expression of a number of cytokine genes is specifically up-regulated in IκBε-null mice, but remarkably not those known to be regulated by p65 and/or c-Rel dimers, such as GM-CSF. The mild phenotype observed for IκBε-deficient mice is probably the result of compensatory mechanisms involving other members of the IκB family, since overexpression of IκBα and IκBβ is observed in several tissues.

Materials and Methods

Design of the targeting construct

A λ DASHII library carrying DNA fragments from a partial *Sau*3A digest of mouse male 129/SV genomic DNA was screened with the entire human *IκBε* cDNA (15). Five bacteriophages spanning a 17.5-kb region encompassing the whole *IκBε* gene were isolated, and their inserts were subcloned into the *Bam*HI site of Bluescript SK^{+} (Stratagene, La Jolla, CA). Restriction mapping and partial sequencing were used to localize *IκBε* encoding regions. A 2.5-kb *Sac*I-*Sma*I fragment containing the 5′ region of the murine *IκBε* gene was subcloned into a derivative of p2ωnlslacZ (kind gift of S. Tajbakhsh, Institut Pasteur, Paris, France), containing a *Xba*I site inserted upstream of the *Nco*I site, giving rise to p5′2ωnlslacZ, a plasmid in which the 5′ region of *IκBε* drives the expression of the *lacZ* gene with an associated nuclear localization sequence (*nlslacZ*). A 1.8-kb Asp^{718}-*Hin*dIII fragment isolated from pPNT (27), which included the HSV-thymidine kinase gene (*HSV-tk*) under the control of the phosphoglycerate kinase (pgk) promoter together with the pgk poly(A), was introduced upstream of the 5′ region of *IκBε*, to generate pPN5′2ωnlslacZ. A 6.6-kb *Bam*HI fragment enclosing the 3′ region of the murine *IκBε* gene was placed upstream of the tk promoter-enhancer driving expression of the diphtheria toxin A-fragment gene (*DTA*) devoid of poly(A) sequences (ptkDaTA, kind gift of S. Tajbakhsh), generating p3′tkDaTA. A 5.5-kb *Nhe*I filled-in *Xho*I fragment from plZ1N (kind gift of S. Tajbakhsh, Institut Pasteur, Paris, France), containing *nlslacZ*, followed by the encephalomyocarditis virus internal ribosome entry site (IRES) upstream of the neomycin-resistance gene (*neo*), was integrated into the *Xho*I-*Eco*RV site of p3′tkDaTA to create plZ1N3′tkDaTA. Finally, an 11.1-kb *Xba*I fragment isolated from pPN5′2wnlslacZ, containing hsvtk, the 5′ region of *IκBε* and *nlslacZ*, was subcloned into the *Xba*I site of plZ1N3′tkDaTA upstream of the IRES, to constitute the final targeting construct.

ES cell transfection and selection

HM1 ES cells (courtesy of David Melton, Edinburgh, U.K.) were grown on primary fibroblast feeder layers in the presence of LIF (10^4 U/ml). A total of 10^7 cells were electroporated with 10 μg of *Not*I-linearized targeting construct in 4-mm cuvettes with a Eurogentec Cellject electroporator at 200 V, 1500 μF, and infinite resistance. Cells were diluted into 40 ml of prewarmed complete medium, plated, and left to recover for 48 h before addition of 0.3 mg/ml G418 (Life Technologies, Cergy, France) with or without gancyclovir at 5 μM. Once established, clones were maintained in complete medium without selection.

Generation and characterization of knockout mice

Two independently targeted ES cell clones were injected into C57BL/6 blastocysts, which were subsequently reimplanted into pseudopregnant C57BL/6 × CBA females. Resulting chimeras were mated to C57BL/6 × DBA/2 mice, and heterozygous offspring for the targeted allele were interbred. The two independent IκBε-null mouse lines generated were found to be identical in all subsequent experiments. Mice were kept in clean housing conditions in a level 2 barrier animal house facility. When unspecified, mice were analyzed between 6 and 12 wk of age.

For Southern blot analysis, genomic DNA was isolated from tail biopsies according to Laird et al. (28). A total of 10 μg of DNA was digested with *Xba*I and *Bam*HI, separated by electrophoresis on 0.9% agarose gel, transferred onto nylon membrane (Amersham Pharmacia Biotech, Amersham, U.K.), and hybridized with a random-primed ^{32}P-labeled 5′ external probe (29).

For genotyping by PCR, tail biopsies were lysed in a buffer containing 50 mM KCl, 10 mM Tris-HCl, pH 8.3, 1.5 mM $MgCl_2$, 0.1 mg/ml gelatin, 0.45% Nonidet P-40, 0.45% Tween 20, and 1 mg/ml proteinase K (Boehringer Mannheim, Meylan, France) at 55°C for at least 3 h. After centrifugation at 14,000 rpm, the supernatant was recovered, heat denaturated at 100°C for 10 min, and used directly in PCR reaction. The forward primer is contained within the 5′ external probe used for Southern analysis (5′-cccgctggacccctggacccc-3′). Two reverse primers were used: one within the first exon of the *IκBε* gene for primer 1 (5′-ccgctcgctctccatccgcatcttctttct-3′), which amplifies the wild-type allele, and a second within the *lacZ* gene (5′-ccgtaaccgacccagcgcccgttgcaccac-3′), which amplifies the mutant allele. PCR reaction mix included 0.25 μM of each of the three primers, 1 mM $MgCl_2$, 0.2 mM dNTP, and 1 U of *Taq* DNA polymerase (Promega, Charbonnières, France). Denaturated samples were subjected to 35 cycles of amplification in a PTC-200 thermal cycler (MJ Research, Cambridge, MA), cycling parameters being the following: 94°C denaturation for 40 s, followed by a combined annealing and polymerization step at 72°C for 4 min. After an extra step at 72°C for 10 min, 10 μl of the reaction was analyzed on a 2.4% agarose gel (containing one-third of NuSieve GTG agarose (FMC) and two-thirds of standard agarose from Life Technologies). Amplified products were detected by ethidium bromide staining.

RNA isolation and Northern blot analysis

Total RNA was isolated from organs or cells using the TRIzol Reagent (Life Technologies), according to the manufacturer's instructions. The RNA pellet was resuspended in nuclease-free H_2O. A total of 30 μg of total RNA was separated by electrophoresis on 1% denaturing formaldehyde agarose gel, transferred onto nylon membrane (Amersham Pharmacia Biotech), and hybridized with a ^{32}P-radiolabeled probe corresponding to full-length human IκBε cDNA.

Western blot analysis and Abs

Whole-cell extracts or cytoplasmic extracts were prepared as previously described (9), and proteins were separated by SDS-PAGE. Proteins were then transferred to nitrocellulose (Schleicher & Schuell, Dasel, Germany) or Immobilon membranes (Millipore, Bedford, MA). Immunoblots were incubated with rabbit polyclonal Abs at 1/1000 dilution (or 1/200 dilution for commercial Abs) and revealed with the Pierce (Rockford, IL) enhanced chemiluminescence system, as recommended by the manufacturer. Sera raised against murine p50 (1263), p65 (1226), p52 (1267), and c-*rel* (1051) were kind gifts of N. Rice (Frederick, MD); serum against RelB was kindly provided by R. Bravo (Princeton, NJ); serum against IκBβ was a generous gift of R. Weil (Institut Pasteur, Paris, France); and sera against IκBα (C-21) and IκBε (M-121) were purchased from Santa Cruz Biotechnology (Santa Cruz, CA).

Cell culture and treatments

Single-cell suspensions of splenocytes or T cells, isolated from thymic suspensions by purification on MACS CD90 (Thy-1.2) MicroBeads (Miltenyi Biotec., Auburn, CA), were cultured at 37°C, 5% CO_2 in RPMI 1640 medium containing 10% heat-inactivated FCS, 100 U/ml penicillin/streptomycin, 2 mM glutamine, and 55 μM 2-ME (all from Life Technologies). Peritoneal macrophages were cultured under the same conditions, but in the absence of 2-ME. LPS from *Salmonella abortus equi* (Sigma, Saint Quentin Fallavier, France), ALLN (Sigma), and murine TNF (R&D Systems, Abingdon, U.K.) were used at 15 μg/ml, 100 μM, and 10 ng/ml, respectively.

Histological analysis and β-galactosidase in situ staining

Organs were fixed for 20–30 min in 4% paraformaldehyde in PBS, incubated in 15% sucrose, 1× PBS for 15 h at 4°C, frozen, and embedded in Tissue-Tek OCT compound (Miles-Bayer). Sections (20 μm) were cut using a cryostat (Leica) and collected on SuperFrost Plus slides (Menzel-Glaser, Germany). Sections were X-gal stained, as previously described (9), and counterstained with eosin. Dehydrated sections were mounted using EUKITT and photographed on a Nikon microscope equipped with a camera, using Kodak Ektachrome 64T film.

Flow cytometric analysis

Single-cell suspensions from thymus, bone marrow, spleen, and lymph nodes were surface stained either with mAbs coupled to fluorescein or PE, or with biotinylated mAbs (PharMingen, San Diego, CA; Caltag, San Francisco, CA), followed by tricolor-streptavidin (Caltag). Viable cells (propidium iodide negative) were then analyzed using a FACScan fluorocytometer (Becton Dickinson, Mountain View, CA). The mAbs used were anti-CD3ε (145-2C11), anti-CD4 (L3T4), anti-CD8 (Ly-3.2 and Ly-2/53-6.7), anti-CD11b/Mac1 (M1/70), anti-CD11c (HL3), anti-CD19 (1D3), anti-CD24/HSA (M1/69), anti-CD25 (7D4), anti-CD43 (S7), anti-CD44 (Ly-24/Pgp-1), anti-CD45R/B220 (RA3-6B2), anti-GR1 (Ly-6G/RB6-8C5), anti-BP-1 (Ly-51/6C3), Ter 119, and anti-IgM (R6-60.2).

For identification of β-galactosidase-expressing cells, lymphocytes isolated by gradient centrifugation through Ficoll-Isopaque (Amersham Pharmacia Biotech) were first stained with a vital fluorogenic substrate, fluorescein-di-β-D-galactopyranoside (FDG; Molecular Probes, Interchim, Montluçon, France), according to Fiering et al. (30). Cells were then washed once before additional immunolabeling and analysis by flow cytometry. Fluorescein background was determined by performing the β-galactosidase assay on lymphocytes isolated in parallel from a wild-type control littermate mouse.

Proliferation assay

Splenocytes (2×10^5/ml) were incubated in the presence or absence of various concentrations of anti-CD3ε (145-2C11), anti-IgM Abs (PharMingen), or LPS. Cells were pulsed with [^{3}H]thymidine (1 μCi/ml; Amersham Pharmacia Biotech) and transferred after 72-h culture onto glass filter mats, and radioactive incorporation was measured with a β-scintillation counter.

Electrophoretic mobility-shift assay (EMSA)

Nuclear extracts from whole organs or T cells, purified by MACS CD90 (Thy-1.2) MicroBeads, were prepared and bandshift assays were performed as previously described (9), using the κB site derived from the promoter of the MHC class I H-2 K^b gene as a probe.

Ig isotype analysis

Sera were prepared from 5- to 6 wk old IκBε$^{-/-}$ and control wild-type sex-matched littermates. Ig isotypes were quantitatively determined against isotype standards using a sandwich ELISA with a pan-specific capture Ab (Southern Biotechnology Associates, Birmingham, AL) and isotype-specific Abs conjugated to alkaline-phosphatase (Southern Biotechnology Associates).

Immunization and T cell-dependent and independent humoral immune responses

Sex-matched animals 5 wk old were immunized by i.p. injection of either 100 μg of KLH coupled to DNP precipitated in alum (T cell-dependent responses) or 50 μg of LPS coupled to DNP (T cell-independent responses). Serum samples were collected from the mice before immunization and at 7-day intervals after immunization for a period of 3 wk. Levels of DNP-specific Ig isotype were determined by ELISA using DNP-BSA (17:1) as a capture agent and goat anti-mouse isotype-specific Abs directly conjugated to alkaline-phosphatase (Southern Biotechnology Associates).

RNase protection assay

Animals 12 wk old were injected i.p. with 2 ml of resazurin-thioglycolate (Sanofi Diagnostics Pasteur, Marnes-la-Coquette, France). After 5 days, peritoneal macrophages were collected from pools of five to six mice and incubated for 8 h at 37°C with or without LPS. Total RNA was then isolated from adherent macrophage cells, as described above, and ribonuclease protection assay was performed with 6 μg of total RNA and the RiboQuant In Vitro Transcription and RPA kits (PharMingen). The murine cytokine sets mCK-2 and mCK-4 (PharMingen) were used to obtain radiolabeled antisense RNA probes for IL-1α, IL-1β, IL-1Ra, IL-3, IL-6, IL-7, IL-11, IL-12p35, IL-12p40, IL-10, IFN-γ, LIF, macrophage migration inhibitory factor, G-CSF, GM-CSF, M-CSF, stem cell factor, L32, and GAPDH. The RNA duplexes were analyzed by electrophoresis on 5% polyacrylamide/8 M urea gels, which were then dried and subjected to autoradiography. Bands were quantified on a PhosphorImager (Molecular Dynamics, Sunnyvale, CA).

Pathogen challenges

Mice 15 wk old were challenged via intranasal injection under ethyl ether anesthesia to 20 μl (1×10^8 bacteria) of a suspension of *Shigella flexneri* strain M90T-GFP, established by M. Rathman (unpublished) and grown as described in Phalipon et al. (31). Mice 12 wk old were inoculated i.v. with 5×10^4 bacteria from *Listeria monocytogenes* EGD strain (32).

At the indicated time after inoculation, lungs were collected from *S. flexneri*-infected mice, or spleen, liver, and brain were removed from *L. monocytogenes*-infected mice. Each organ was homogenized with an Ultraturrax blender in sterile saline solution. For each organ, bacteria were titrated by serial dilutions plated on Congo red agar (infection by *S. flexneri*) or BHI agar (infection by *L. monocytogenes*) and incubated at 37°C. Results were expressed as the number of CFU per gram of lung tissue for *S. flexneri* and as the logarithm of CFU per organ for *L. monocytogenes* infection.

Results

Generation of IκBε-deficient mice

To inactivate the murine *IκBε* gene by homologous recombination in ES cells, we cloned a 17.5-kb genomic region encompassing the *IκBε* gene from a 129/SV library, using the human *IκBε* cDNA as a probe (15). The targeting construct was designed (Fig. 1*A*) to replace the entire coding sequence of *IκBε*, starting from the ATG, by *nlslacZ* to follow the expression pattern of *IκBε* in vivo (33). The construct contains a promoterless *neo* gene (34), positioned downstream of *nlslacZ*, and whose translation is dependent on the presence of an upstream IRES (35). *Hsv-tk* and *DTA* were placed at each end of the construct to achieve a double-negative selection (36, 37). We checked that *IκBε* mRNA was detectable in ES cells, even if it was at very low levels compared with those of *IκBβ* or *IκBα*, this latter constituting the major IκB species in these cells (data not shown). By transient transfection experiments into ES cells, we also verified that the 2.5-kb 5′ fragment used in the targeting construct was unable to drive *nlslacZ* gene expression by itself (data not shown). Following electroporation of the targeting vector into HM1 ES cells, G418-resistant colonies obtained in the presence or absence of gancyclovir were selected and screened by

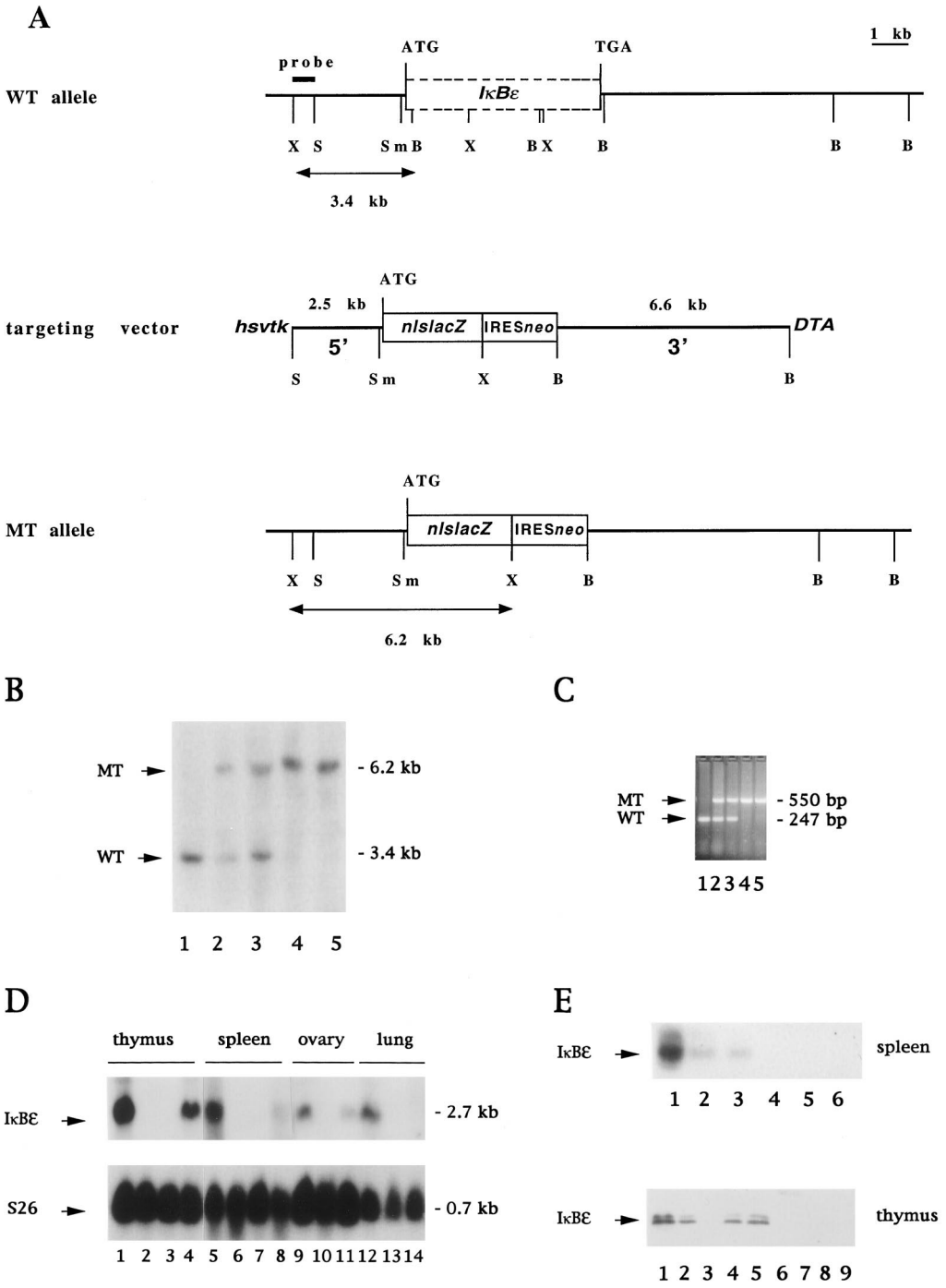

FIGURE 1. Generation of IκBϵ-deficient mice. *A*, Schematic representation of the wild-type (WT) and mutated (MT) genomic *IκBϵ* loci together with the targeting vector. Restriction enzyme sites (B, *Bam*HI; S, *Sac*I; Sm, *Sma*I; X, *Xba*I) and the probe for Southern analysis are indicated. The precise position of the exons in the genomic DNA is unknown. Homologous recombination of WT DNA with the targeting construct results in the replacement of all *IκBϵ* coding sequences with *nlslac*ZIRES*neo* sequences. *B*, Southern blot analysis of DNA preparations from tails of adult mice from heterozygote matings. The three genotypic categories obtained correspond to wild-type (*lane 1*), heterozygote (*lanes 2* and *3*), and homozygote (*lanes 4* and *5*). Digestion of genomic DNA with *Bam*HI plus *Xba*I, followed by hybridization with the 5′ external probe depicted above, generates a 3.4-kb fragment for the wild-type (WT) allele and a 6.2-kb fragment for the mutated (MT) allele. *C*, PCR analysis of the DNA samples used in *B*. Design of primers allows the amplification of a 247-bp fragment for the wild-type (WT) allele and a 550-bp fragment for the mutated (MT) allele. *D*, Northern blot analysis of total RNA from wild-type, heterozygous, and homozygous mutant IκBϵ mice. Total RNA (30 μg) extracted from the thymus (*lanes 1–4*), spleen (*lanes 5–8*), ovary (*lanes 9–11*), or lung (*lanes 12–14*) was electrophoresed and transferred to nylon membrane. *Top panel*, Hybridization with full-length human IκBϵ cDNA. Autoradiography for thymus and spleen has been exposed 2.5-fold less than that for ovary and lung. *Bottom panel*, The same filter was rehybridized with a S26 probe (68). *Lanes 1*, *5*, *9*, and *12*, Wild-type; *lanes 4*, *8*, and *11*, heterozygotes; *lanes 2*, *3*, *6*, *7*, *10*, *13*, and *14*, homozygous mutants. *E*, Western blot analysis of protein extracts from wild-type, heterozygous, and homozygous mutant IκBϵ mice. Total extracts from spleen (200 μg) (*top panel*) or thymus (100 μg) (*bottom panel*) were examined by immunoblot analysis with a polyclonal Ab directed against IκBϵ. *Top panel* (spleen), *lane 1*, wild type; *lanes 2* and *3*, heterozygotes; *lanes 4*, *5*, and *6*, homozygous mutants. *Bottom panel* (thymus), *lanes 1* and *5*, wild type; *lanes 2* and *4*, heterozygotes; *lanes 3*, *6*, *7*, *8*, and *9*, homozygous mutants. Densitometry scanning of bands in *bottom panel*, thymus, *lane 5* indicates a more intense signal compared with that observed for *lanes 3* and *4*.

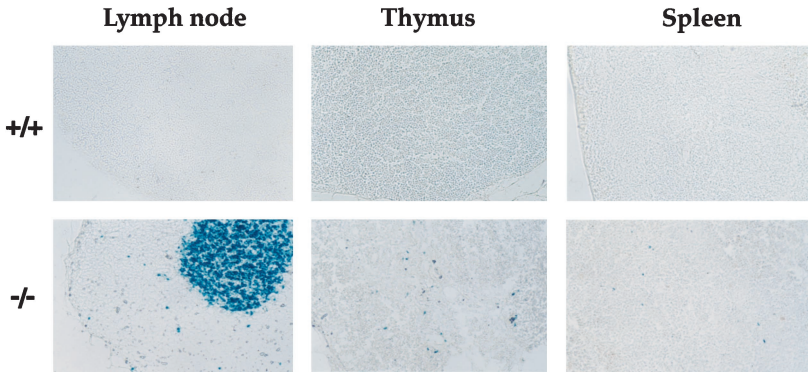

FIGURE 2. Histological examination of lymphoid organs of IκBε-deficient mice. Thymus, spleen, or lymph node sections of adult wild-type (+/+) or IκBε-null (−/−) mice were stained with X-gal for *lacZ* expression and counterstained with eosin (×200 magnification).

Southern blot analysis. Of 42 recombinant ES clones examined, 9 were positive for homologous recombination and 1 of these 9 clones harbored an additional insertion in the genome, as evidenced by probing with a *lacZ* fragment (data not shown). Selection in the presence or absence of gancyclovir yielded the same percentage of homologous recombinant clones, indicating that *DTA* alone was sufficient for negative selection. Two correctly targeted clones from two independent electroporations were injected into C57BL/6 blastocysts and gave rise to chimeric mice that displayed 100% color chimerism and that all transmitted the recombinant allele to their progeny (with one exhibiting 50% germline transmission). Two independent IκBε mutant mouse lines were thus established, analyzed in parallel, and found to be indistinguishable in all subsequent experiments. Intercrossing heterozygous animals, which displayed no obvious phenotype, generated IκBε$^{+/+}$, IκBε$^{+/-}$, and IκBε$^{-/-}$ mice, identified by Southern blot and PCR analysis (Fig. 1, *B* and *C*). IκBε expression was abolished in homozygous mutants, as determined by Northern blotting with total RNA purified from several organs (Fig. 1*D*) and Western blot analysis of spleen and thymus total protein extracts (Fig. 1*E*). Intermediate levels of IκBε mRNA or protein were observed in every heterozygote organ examined (Fig. 1*D*, *lanes 4*, *8*, and *11*, and Fig. 1*E*, *lanes 2* and *3*, spleen; and *lanes 2* and *4*, thymus), indicating that both *IκBε* alleles are functional in wild-type mice. IκBε$^{-/-}$ mice were born at the expected Mendelian segregation ratios and grew normally. No evident morphological or behavorial abnormalities were detected. IκBε-null mice did not show any gross macroscopic alterations either, as determined by detailed histopathological analysis, and their skeleton appeared indistinguishable from that of wild-type mice by x-ray irradiation and Alcian blue/Alizarin red staining (data not shown).

Normal histology of lymphoid organs of IκBε-deficient mice

Examination of tissue sections from thymus, spleen, or lymph nodes of wild-type (+/+) or homozygous mutant (−/−) mice did not display any significant differences (Fig. 2). In situ staining of these sections by X-gal, a colorimetric substrate for β-galactosidase, was used to elucidate the expression pattern of *IκBε* in these organs, the *nlslacZ* gene having been knocked in to the *IκBε* locus and thus placed under the control of the endogenous *IκBε* regulatory sequences. X-gal staining revealed that the major site of *IκBε* expression is the lymph node, and especially the medulla. *LacZ* expression is scattered throughout the thymus and restricted to a few cells in the spleen (Fig. 2). Further characterization of the β-galactosidase-expressing cells was performed by flow cytometry with simultaneous detection of surface Ags and fluorescent staining of β-galactosidase using the FDG fluorogenic vital substrate (38). Results presented in Table I show that the highest number of FDG$^+$ cells is located within the lymph node (50%) and decreasingly in the thymus (30%) and the spleen (5%), corroborating the in situ staining data. Interestingly, in each organ, T cells constitute the major FDG$^+$ species. Some B cells (between 4 and 15% of FDG$^+$ lymphocytes) also exhibit β-galactosidase activity in the two secondary lymphoid organs examined. Immunolabeling of lymph node cells with Mac1, GR1, or CD11c did not reveal any specific FDG$^+$ population, the number of immunolabeled and

Table I. *Identification of lymphocyte subsets expressing* IκBε *by FACS analysis of FDG-stained and immunolabeled lymphocytes from IκBε-mutant mice*[a]

		CD3$^+$ (%)	CD4$^+$ (%)	CD8$^+$ (%)	CD4$^+$ CD8$^+$ (%)	B220$^+$ (%)
Thymus	FDG$^+$ (30%)	91	6.3	1.3	92	–
	FDG$^-$ (70%)	93	5.5	2.5	89	–
Spleen	FDG$^+$ (5%)	82	47	34	–	15
	FDG$^-$ (95%)	25	16	10	–	70
Lymph nodes	FDG$^+$ (50%)	92	65	26	–	4
	FDG$^-$ (50%)	55	31	18	–	45

[a] Percentages of cells, isolated from the thymus, spleen, or lymph nodes of IκBε-mutant heterozygote mice, expressing β-galactosidase activity vs. CD3, CD4, CD8, B220 immunolabeling are presented. In brackets are indicated percentages of FDG$^+$ or FDG$^-$ cells vs total lymphocyte population. Percentages represent the means of four heterozygote mutant mice. Similar values were obtained for homozygous mutant mice (data not shown).

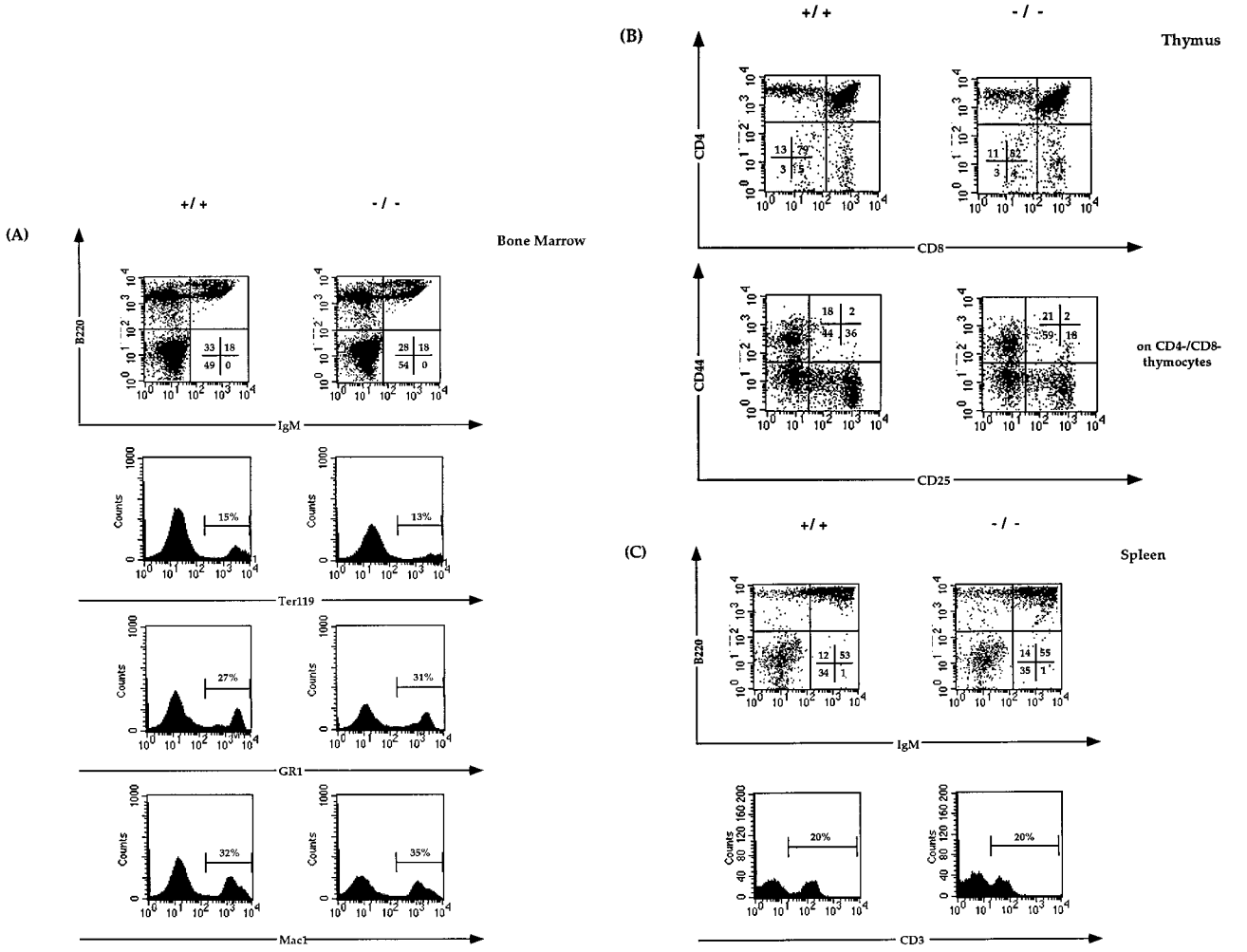

FIGURE 3. Expression pattern of immune cell surface markers in IκBϵ-deficient mice. Bone marrow cells (*A*), thymocytes (*B*), and spleen (*C*) lymphocytes isolated from adult wild-type (+/+) or IκBϵ-null (−/−) mice were analyzed by flow cytometry. Single-cell suspensions were prepared from the organs described and stained with fluorochrome-conjugated Abs to IgM, B220, CD4, CD8, CD44, CD25, CD3, Ter119, GR1, or Mac1. The percentage of total cells is indicated in each quadrant of the different dot plots.

FDG^+ cells being 1.5%, 4%, and 1%, respectively (data not shown).

Normal mature hemopoietic cell populations and diminution of one T cell precursor subset in IκBϵ-deficient mice

We next investigated whether hemopoietic cell populations were normal in IκBϵ-null mice. Results from flow cytometric analyses of bone marrow, thymic, and splenic cell populations are presented in Fig. 3. No difference between the wild-type (+/+) and the homozygous mutant (−/−) mice was observed in the expression of B cell Ags (B220, IgM), erythroid cell Ag (Ter119), granulocyte Ag (GR1), and macrophage Ag (Mac1) in the bone marrow (*A*), or B cell Ags (B220, IgM) and T cell markers (CD3) in the spleen (*C*). We also tested surface markers for precursor B cells according to the classification of Hardy (39), such as CD43, HSA, CD19, BP-1 in the bone marrow, markers for dendritic cells like CD11c in the spleen, and markers for granulocytes, GR1, and macrophages, Mac1, in the lymph nodes (data not shown). No significant differences were detected between wild-type and mutant animals. In the thymus (*B*), the percentage of CD4, CD8 double or simple positive cells are identical in both types of mice. Remarkably, when we examined the expression of CD44 and CD25 in the $CD4^-/CD8^-$ population, we observed a 50% fold reduction in the percentage of $CD44^-/CD25^+$ cells in IκBϵ-null mice compared with control wild-type littermates, the other populations being normal. Peripheral blood analysis of IκBϵ-deficient mice revealed a standard cell count for every cell population, other hemogram parameters being average (data not shown). Overall, these results establish the presence of normal numbers of mature B cells, T cells, erythroid cells, dendritic cells, granulocytes, and macrophages in IκBϵ mutants even though one precursor T cell subspecies is diminished.

Normal proliferation of splenocytes from IκBϵ-deficient mice in response to mitogenic stimuli

We next investigated whether splenocytes from wild-type (+/+), heterozygote (+/-), or IκBϵ-null (−/−) mice responded normally to various mitogens known to induce B and/or T cell proliferation via distinct signaling pathways. Results presented in Fig. 4 reveal no significant difference in the proliferative response of the splenocytes derived from these three genotypes to anti-CD3 (*A*), LPS (*B*), or anti-IgM (*C*), albeit large variations were observed among individuals.

We then asked whether the mild phenotype observed for IκBϵ-deficient mice could be due to compensatory mechanisms involving up-regulation of other IκB family members. We thus assessed the levels of other IκB molecules in the spleen of IκBϵ-null (−/−)

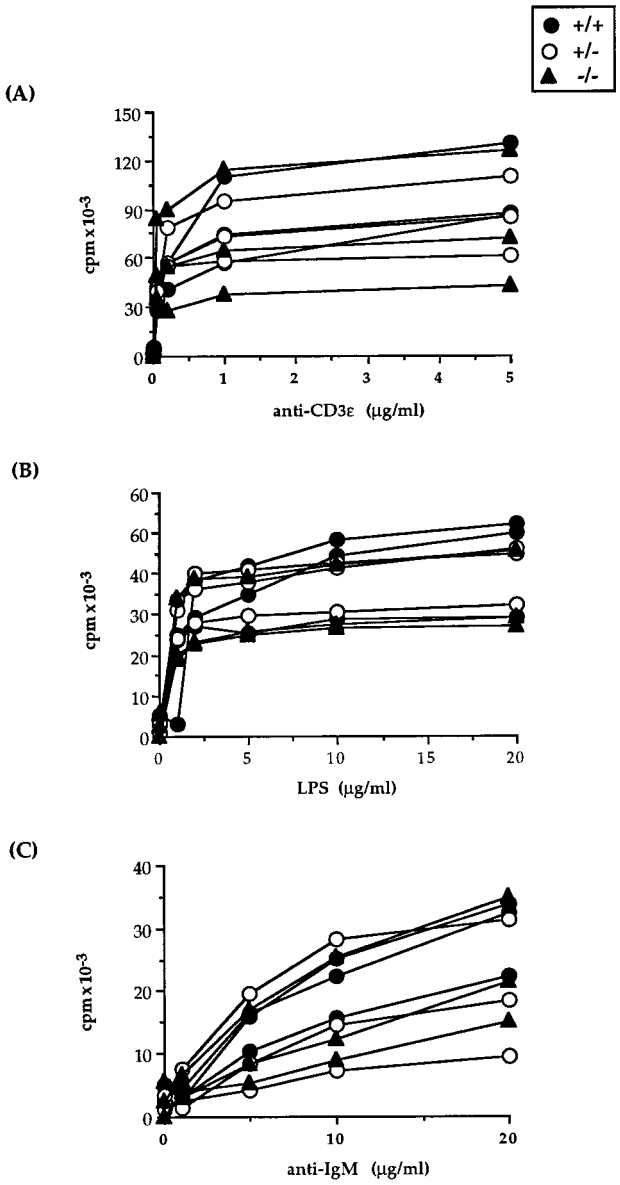

FIGURE 4. Normal proliferation of splenocytes from IκBε-deficient mice in response to mitogenic stimuli. Splenocytes from wild-type (+/+), heterozygote (+/−), or IκBε-null (−/−) mice were incubated with increasing concentrations of anti-CD3 (*A*), LPS (*B*), or anti-IgM (*C*) for 72 h at 37°C. Proliferation was measured by [^{3}H]thymidine incorporation.

mice. A representative Western blot analysis of total splenic extracts of wild-type (+/+) and IκBε-null (−/−) mice is presented in Fig. 5 ($n = 4$). In IκBε-deficient mice, increased levels of IκBα and IκBβ were observed, whereas expression of p105 and p100 was not significantly affected (*A*). As expected, IκBε, found in wild-type cells, was absent in the homozygous mutant cells (*A*, *upper panel*). Since the synthesis of three members of the NF-κB family, p105, p100, and c-Rel, is directly controlled by NF-κB itself (2, 6), we also looked at the expression of p50, p65, c-Rel, and RelB (*B*). The steady state levels of all these molecules were similar in IκBε-deficient and wild-type mice. This latter result together with the observed up-regulation of IκBα and IκBβ suggests that constitutive nuclear NF-κB activity may be unchanged in IκBε-deficient mice. This was shown to be the case when we performed bandshift assays with nuclear extracts from the spleen or resident macrophages of homozygous mutant or control wild-type littermate mice (data not shown).

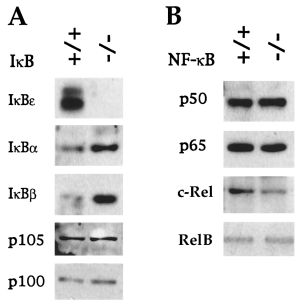

FIGURE 5. NF-κB and IκB family members expression in adult IκBε-null mice. Total extracts (120 μg) from the spleen of wild-type (+/+) or IκBε-deficient (−/−) mice were analyzed by Western blot analysis with polyclonal Abs directed against p50, p65, c-Rel, RelB, IκBα, IκBβ, and IκBε. Double loading of the protein extracts on a unique gel, transferred to a single Immobilon membrane that had been cut in pieces, was used to allow incubation of the different Abs on comparable blots.

Normal TNF response of T cells from IκBε-deficient mice

Since *IκBε* is preferentially expressed in T cells (see above), we examined how mutant T cells responded to TNF treatment. Thymocytes purified from wild-type (+/+) (*lanes 1–5*), heterozygote (+/−) (*lanes 6–10*), or IκBε-deficient (−/−) (*lanes 11–15*) mice were incubated with TNF for various periods of time in the absence (*lanes 1–4*, *6–9*, and *11–14*) or in the presence of ALLN (*lanes 5*, *10*, and *15*) (Fig. 6). Analysis of nuclear extracts by EMSA (*A*) showed a similar overall response of the cells isolated from the three categories of mice: we observed no modification of constitutive NF-κB DNA-binding activity nor of the kinetics of activation after TNF stimulation. ALLN treatment through inhibition of the proteasome prevented induction in a comparable fashion in all three genotypes. The use of specific Abs directed against individual members of the NF-κB family allowed us to define complex II as p50/p50 homodimers and complex I as p50/p65 heterodimers (data not shown). Analysis of cytoplasmic extracts by Western blotting (*B*) confirmed the absence of IκBε in T cells of homozygous mutant mice (*bottom panel*). No increase of p105 and IκBβ was detected in mutant thymocytes (*upper panels*). IκBβ was not degraded after TNF treatment in either wild-type or IκBε-deficient T cells. IκBα was up-regulated in resting mutant thymocytes, and rapidly degraded and resynthesized after TNF treatment. Its degradation was inhibited by ALLN in both mutant and wild-type or heterozygous control cells. Stimulation of T cells with IL-1 again did not discriminate between mutant and control cells (data not shown).

Altered resting and Ag-specific Ab production in IκBε-deficient mice

To assess the humoral immunity of IκBε-null mice, we measured basal Ig levels of naive mutant mice or control wild-type littermates (Fig. 7*A*). IgG2a, IgG2b, and IgG3 levels are equivalent in both types of mice. A slight increase of IgM levels (2-fold) is detected in IκBε-deficient mice compared with in control mice. The main difference between these mice lies in the augmentation (3-fold, with very small dispersion of the values obtained with the mutant mice, $p < 0.001$) of IgG1 seen in IκBε-deficient mice compared with wild-type mice.

We next analyzed the humoral response of IκBε-null mice or control wild-type littermates to specific Ab challenge. Mice were injected with LPS coupled to DNP to induce a T cell-independent response (*B*) or with KLH coupled to DNP precipitated in alum to induce a T cell-dependent response (*C*) and bled before and 7, 14,

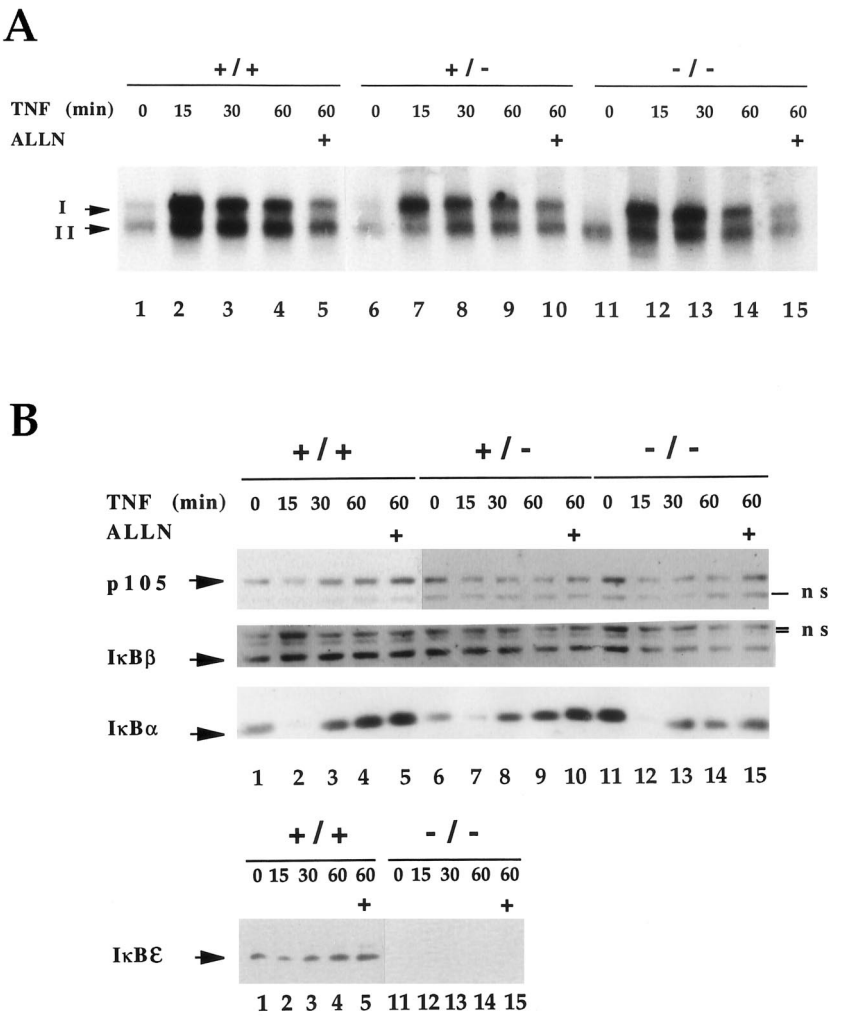

FIGURE 6. Normal TNF response of purified T cells from IκBε-deficient mice. T cells from wild-type (+/+) (*lanes 1–5*), heterozygote (+/−) (*lanes 6–10*), or IκBε-null (−/−) (*lanes 11–15*) mice were purified by MACS CD90 (Thy-1.2) MicroBeads and incubated for the indicated periods of time at 37°C in the presence of TNF (10 ng/ml) with (*lanes 5*, *10*, and *15*) or without ALLN (100 μM, added 30 min before TNF). Nuclear and cytoplasmic extracts were then prepared and used in bandshift assay or Western blot analysis, respectively. For EMSA, nuclear extracts (5 μg) were incubated with a double-stranded oligonucleotide corresponding to a canonical κB site located in the promoter of the MHC class I gene H-2 K^b. Arrowheads point out the different NF-κB/Rel complexes discussed in the text. For Western blot analysis, 40 μg of cytoplasmic extract per lane was separated by SDS-PAGE, and transferred to Immobilon. The membrane was cut and pieces were probed with polyclonal Abs directed against p50, IκBα, or IκBβ. The same cytoplasmic extracts were used for a blot incubated with polyclonal Ab directed against IκBε. Nonspecific bands (ns) are indicated.

and 21 days after immunization. DNP-specific Abs in unchallenged mice were very low and not significantly different in wild-type and mutant mice. For each Ag used, only DNP-specific IgG1 and IgM isotype productions were affected in IκBε-null mice; IgG2a, IgG2b, and IgG3 values were not statistically different from the wild-type values using the Student's test.

Considering the T cell-independent response (*B*), DNP-specific IgG1 production in mutant mice increased by 3-fold at day 7, and this elevation persisted until day 21. DNP-specific IgM synthesis in the mutant mice was 2-fold higher at day 7 and 1.3-fold at day 14, and returned to levels similar to wild type at day 21.

For the T cell-dependent response (*C*), DNP-specific IgG1 secretion in IκBε-deficient mice differed from wild type only by a peak (1.5-fold increase) at day 7. DNP-specific IgM production rose by 2.5-fold at day 7 and remained elevated until day 21.

Constitutive up-regulation of cytokines in IκBε-deficient mice

Analysis of IκBε-associated proteins in cells, together with the finding that some NF-κB-responsive genes were activated solely by c-*rel* and/or p65 dimers, led to the hypothesis that the role of IκBε in vivo might be to regulate this specific subset of genes, which includes IL-8, tissue factor, and GM-CSF (15, 17). If this assumption true, these genes should have elevated basal expression levels in IκBε-deficient mice. Since some of these genes are inducible in activated macrophages (40), we examined the expression of an array of cytokines in thioglycolate-elicited macrophages (Fig. 8) in the absence (*lanes 1*, *2*, *3*, *7*, *8*, and *9*) or presence of LPS for 8 h (*lanes 4*, *5*, *6*, *10*, *11*, and *12*). Total RNA was purified and subjected to RNase mapping for the expression of different chemokine genes. The expression of IL-1α, IL-1β, IL-1Ra, and to a lesser extent IL-6 was constitutively increased in IκBε-deficient mice (*A*, *lanes 3* and *B*, *lane 9*), while their mRNA levels were below detection (for IL-1β and IL-6) or very low (for IL-1α and IL-1Ra) in wild-type and heterozygote mutant mice ($n = 5$) (*A*, *lanes 1* and *2*, and *B*, *lanes 7* and *8*). Remarkably, GM-CSF expression remained unaffected and undetectable in the mutant mice (*B*, *lane 9*). Upon LPS stimulation, comparable fold induction of IL-1α, IL-1β, IL-1Rα, IL-6, IFN-γ, GM-CSF, and G-CSF expression was observed in mutant and control mice (*A*, *lanes 4*, *5*, and *6*, and *B*, *lanes 10*, *11*, and *12*).

Normal response to pathogen challenge in IκBε-deficient mice

It has been previously shown that IL-8, monocyte chemoattractant protein-1, GM-CSF, TNF, and IL-6 were specifically up-regulated upon bacterial invasion of human colonic epithelial cells (41, 42), and that the induction of expression of IL-8 and monocyte chemoattractant protein-1 in HUVEC following infection with *L. monocytogenes* was directly correlated with the activation of NF-κB (43). If GM-CSF or the functional equivalent of IL-8 in the mouse was constitutively overexpressed in IκBε-deficient mice, one should expect, in a simplistic view, a quicker clearance of pathogenic bacteria. We thus asked how IκBε-null mice responded

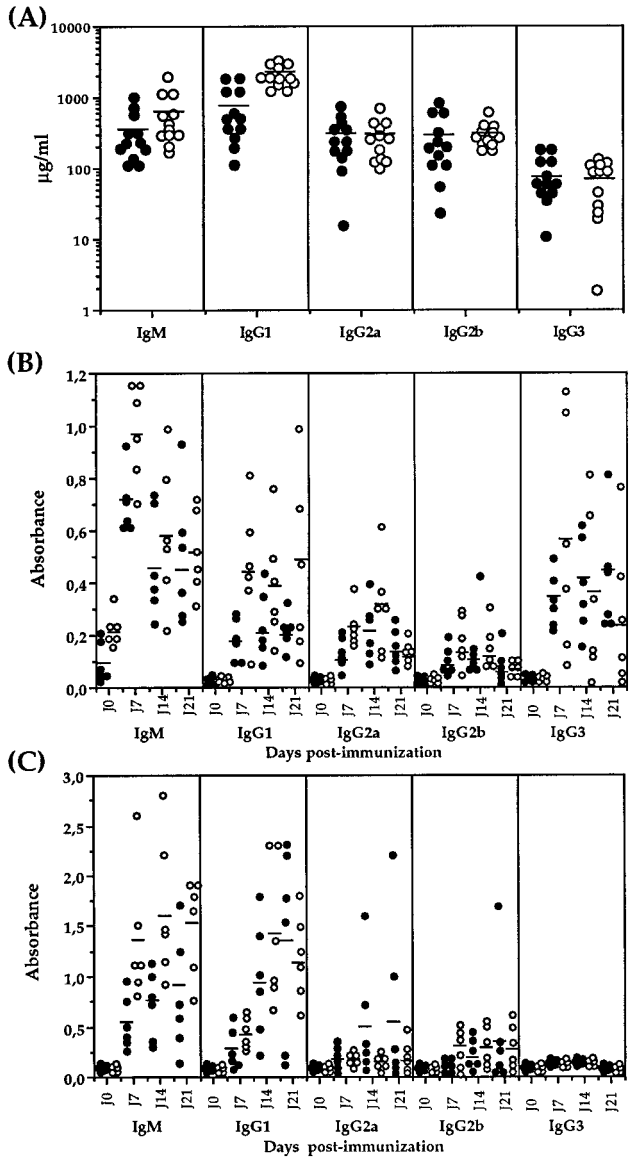

FIGURE 7. Increased production of IgG1 Ig isotype in unimmunized IκBε-deficient mice and altered humoral immune response to T cell-dependent and T cell-independent Ags in IκBε-deficient mice. Serum Ig levels from wild-type (closed circles) or IκBε-null (open circles) mice were measured by isotype-specific ELISA. Twelve animals per group were used for unimmunized mice (*A*), and six animals per group for mice immunized with a T cell-independent (*B*) or T cell-dependent Ag (*C*). Serum samples from mice immunized with 50 μg of DNP-LPS (*B*) or 100 μg of DNP-KLH (*C*) were collected before immunization, and after 7, 14, and 21 days. Horizontal lines indicate the mean values.

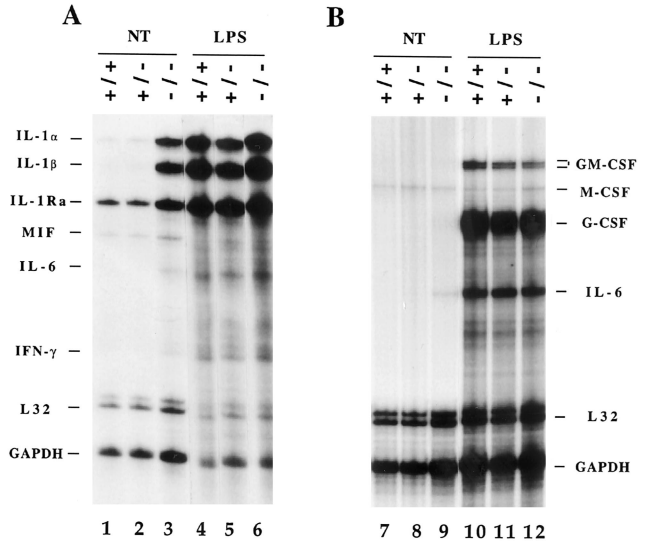

FIGURE 8. Constitutive induction of IL-1α, IL-1β, IL-1Ra, and IL-6 mRNA synthesis in IκBε-deficient mice. Thioglycolate-elicited macrophages were recovered from wild-type (+/+) (*lanes 1, 4, 7,* and *10*), heterozygote (+/−) (*lanes 2, 5, 8,* and *11*), or IκBε-null (−/−) (*lanes 3, 6, 9,* and *12*) mice and incubated for 8 h at 37°C in the absence (*lanes 1, 2, 3, 7, 8,* and *9*) or in the presence of LPS (15 μg/ml) (*lanes 4, 5, 6, 10, 11,* and *12*). Total RNA was then prepared, and 6 μg was used for cytokine mRNA quantitation by RNase protection assay with the multiprobe template sets mCK-2 (*A*) and mCK-4 (*B*) (PharMingen), as described in *Materials and Methods*. Each lane is representative of five to six mice, and the experiment was repeated four times with consistent results. L32 and GAPDH are internal control RNAs present at equivalent amounts in each sample assayed. They served to normalize each cytokine mRNA level. When referred to these internal control bands, the faint band for IFN-γ observable in *lane 3* is not significant and was never observed in four other independent samples.

to challenge with a Gram-negative, *S. flexneri*, or with a Gram-positive, *L. monocytogenes*, bacteria. We used a previously described pulmonary model of *Shigella* infection by the nasal route, which mimics the lesions occurring in natural intestinal infection (31). As shown in Fig. 9*A*, high bacterial multiplication was observed in the lungs of wild-type mice 6 h after inoculation, the bacterial load decreasing after 24 h. An overall similar pattern of response to *S. flexneri* was obtained with heterozygote or homozygous IκBε mutant mice, the high SD between individual animals observed at 24 h ruling out any significant effect in the mutant mice. We next challenged the mice with *L. monocytogenes*. Results presented in Fig. 9*B* show that for every organ analyzed (liver, spleen, and brain), IκBε-null mice responded to the infection identically in intensity and kinetics to wild-type or heterozygote controls. This absence of bias between these three populations of mice persisted when we looked at the spleen 6 days after inoculation when bacterial loads were considerably diminished (data not shown). By using two distinct bacterial pathogens, one which led to localized bronchial epithelium invasion, and a second, which caused a systemic infection that ended in CNS invasion, we have been unable to establish any discrimination between the mutant and the wild-type control mice.

Discussion

The existence of three major IκBs raises the question of their individual role and putative functional redundancy in vivo. The analysis of IκBε-deficient mice provides some clues about the function of IκBε in a whole organism. IκBε-null mice share none of the hallmarks of IκBα-deficient mice (23, 44): they survive to adulthood and show no increase in NF-κB DNA-binding activity in all organs and cell types analyzed (spleen, thymus, purified T cells, resident macrophages, or MEFs (data not shown)). They possess normal hemopoietic cell subsets, in particular displaying average granulocyte and macrophage numbers together with unaltered skin structure.

We have shown in this study that IκBε mRNA is expressed at high levels in the thymus, spleen, and to a lesser extent in lung and ovary, in accordance with observations in humans (16). Targeted replacement of the entire *IκBε* coding region by the *lacZ* gene carrying a nuclear localization sequence allowed us to visualize the overall expression pattern of IκBε in the immune system with

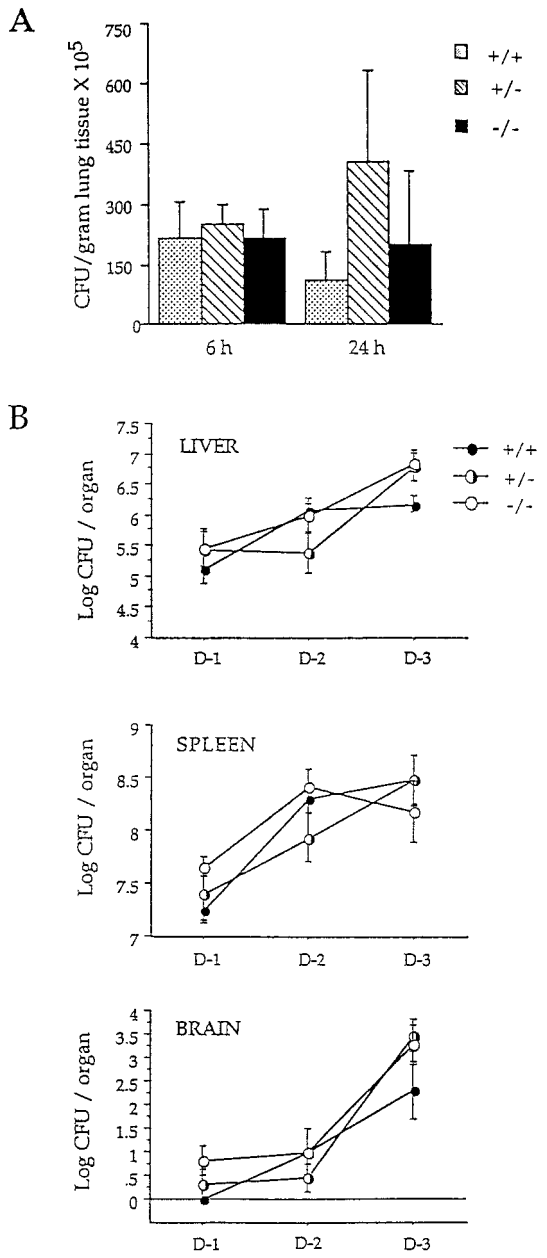

FIGURE 9. Normal responses of IκBε-deficient mice after pathogen challenge. *A*, 7 to 23 wild-type (+/+), heterozygote (+/−), or IκBε-null (−/−) mice were intranasally infected with *S. flexneri*, lungs were removed after 6–24 h, and the bacterial load was assessed. Results are expressed as the means + SD of CFU/gram of lung tissue from every inoculated mice. *B*, 5 to 7 wild-type (+/+), heterozygote (+/−), or IκBε-null (−/−) mice were i.v. infected with *L. monocytogenes*. Spleen, liver, and brain were removed after 1, 2, or 3 days (D-1, D-2, and D-3, respectively), and the bacterial load was assessed. Results are expressed as the mean + SD of the log of CFU/organ from every inoculated mouse.

cellular resolution. Analysis of β-galactosidase expression by in situ X-gal staining or by FACS analysis of FDG-labeled cells confirmed our Northern blotting data and revealed that IκBε-expressing cells represent one-half of the cells in the lymph node, one-third in the thymus, and only 5% in the spleen. β-galactosidase-positive cells are mostly T cells, in every primary or secondary lymphoid organ examined. A small fraction of macrophages (1.5%), granulocytes (4%), dendritic cells (1%), and B cells (1–2%, depending on the organ) expresses IκBε. These results indicate that data from cell lines of the myeloid lineage, like THP1 or differentiated HL-60 cells, which display high endogenous levels of IκBε (15), cannot be extrapolated to primary cells. Considering the high sensitivity of FDG staining, which has been reported to detect as little as five molecules of β-galactosidase per cell (38, 45), and the fact that two independently generated knockin lines gave the same pattern of expression, it is quite unlikely that we overlooked any site of expression of IκBε in the lymphoid system.

Up-regulation of IκBα has been observed in several organs and cell types (i.e., thymus, spleen, purified T cells) isolated from IκBε-mutant mice. IκBβ was found overexpressed in the spleen, but not in purified T cells. These results suggest that the relative contributions of IκBα and IκBβ to the regulation of NF-κB are cell type dependent. The prominent role of IκBα is most likely due to its preferential expression in hemopoietic cells compared with IκBβ (44) and also to its autoregulation by NF-κB (46–50). IκBε expression is controlled by NF-κB, and IκBε protein levels are increased in primary IκBα-null MEFs (15). Up-regulation of other IκB species is therefore not a characteristic unique to IκBε-null mice. However, up-regulation of IκBα and IκBβ in the spleen of IκBε-nullizygous mice is intriguing since only 5% of FDG^+ cells were detected in this organ. It may suggest that overexpression of IκB family members could also take place in cells that do not normally express IκBε.

No significant increase in NF-κB-binding activity was detected in any IκBε-deficient organs examined or in purified T cells, of which 80% express IκBε. This suggests that cytoplasmic retention of NF-κB in IκBε-deficient mice is achieved by overexpression of IκBα and/or IκBβ. This functional compensation by IκBα and/or IκBβ for the lack of IκBε is most likely responsible for the discrete phenotype of IκBε-null mice. Nevertheless, substitution by these IκBs is not complete and IκBε-deficient mice harbor a number of specific features, which might reflect specific functions of IκBε.

We observed a 50% decrease in the number of precursor $CD44^-CD25^+$ cells in spite of the presence of normal mature hemopoietic cell populations. Differentiation of thymocytes has been correlated with CD25 and CD44 expression during early steps of cortical maturation (51), and CD25 (or IL-2Rα-chain) expression in thymocytes is associated with TCR rearrangement. It is interesting to note that young mice lacking CD25 exhibit phenotypically normal T cell development (52). Lack of IκBε may impair expression of target genes involved into the proliferation of the $CD44^-CD25^+$ cell population and thus account for its diminution. Whereas CD25 gene expression was unaffected in IκBα-null mice (23, 44) and in homozygous mice deficient for the different members of the NF-κB/Rel family (53–59), a similar reduction in the frequency of $CD25^+$ cells was detected in transgenic mice expressing constitutive *trans*-dominant form of IκBα (26). Reduction of the $CD25^+$ cell population in IκBε-deficient mice might therefore result from an increase of IκBα, instead of being a direct consequence of IκBε loss. In this case, the up-regulation of IκBα should be assumed to be strictly limited to the $CD25^+$ cell subset, since in IκBα transgenic mice this phenotype is associated with severe defects in T cell development and proliferation that are not observed in IκBε-null mice.

Another characteristic of IκBε-deficient mice is their increase in IgM and especially IgG1 basal levels. Recent reports have implicated NF-κB in the regulation of isotype switching. κB binding sites within the 3′ IgH enhancer (60, 61) and the germline C_H promoters, which regulate class switching to IgG1 and IgE (62, 63), were shown to bind specific NF-κB complexes, and analysis of the knockouts of the various NF-κB genes led to the observation that isotype switching was frequently affected in these mice. For instance, p50 mice displayed a significant reduction in all isotypes

except for IgM, which was slightly elevated (55). A pronounced reduction of IgG1 and IgA was seen in p65-deficient lymphocytes (56). RelB-deficient mice show increases in IgM, IgE, and IgG1 together with slight decreases in IgG2a, IgG2b, IgG3, and IgA (64). IgG1 and IgG2 were drastically reduced in c-Rel-null mice, IgM, IgG2b, and IgG3 being only slightly diminished (53). IgG1 and IgM levels appear to be frequently altered in NF-κB-deficient mice, and their increase in IκBε-null mice might reflect modification of the balance of various NF-κB members in B cell subsets. Ab response to specific Ags was also modified in IκBε-deficient mice. T cell-dependent and T cell-independent immunizations led to increased synthesis of IgM and IgG1. Impaired Ag-specific Ig isotype switching has also been observed in several NF-κB-deficient mice. C-Rel and RelB knockout mice exhibit defective T-dependent and T-independent Ab responses (53, 64), while an inability to generate Abs to T-dependent Ags has been observed in p52-null mice (58, 59). The increase in IgM and IgG1 levels before stimulation and after T-independent or T-dependent challenge in IκBε-nullizygous mice is, however, very modest compared with the perturbation observed for knockouts of the NF-κB gene family. Moreover, we have shown that only 1–2% of B cells express IκBε. Alteration of isotype switching in IκBε-deficient mice possibly reflects the contribution of these few IκBε-expressing B cells. Alternatively, it is possible that this modification is indirectly due to IκBε via the perturbation of other pathways such as cytokine synthesis.

IκBε was proposed to be a specific regulator of genes controlled by p65 and/or c-Rel complexes, since it specifically interacts with p65 and/or c-Rel-containing complexes (15), and inhibits transcription of the human IL-8 gene, which is only activated by p65 homodimers (17). Analysis of basal cytokine mRNA levels in thioglycolate-elicited macrophages revealed that expression of κB-responsive genes, such as IL-1α, IL-1Rα, IL-6, or IL-1β, which binds p50/p65 dimers (65, 66), was up-regulated in IκBε-deficient mice. On the contrary, expression of the GM-CSF gene that binds only p65/c-Rel heterodimers in vitro (67) remains undetectable, as does IFN-γ and G-CSF expression. mRNA levels of G-CSF, macrophage-inflammatory protein-2 (a mouse IL-8 homologue), and VCAM-1 were elevated in IκBα-deficient thymocytes, in constrast to GM-CSF, IL-2, IL-2Rα, and IL-6 (44). These data indicate that different cytokine genes may be controlled by distinct IκBs, and that IκBε may not function in vivo as a specific inhibitor of genes specifically regulated by p65 and/or c-Rel complexes. This assumption is supported by normal responses of IκBε-deficient mice to pathogen challenge involving IL-8 and GM-CSF at the onset of infection (41–43).

Functional redundancy and up-regulation of other IκB members mask the full importance of IκBε in vivo and explain the mild phenotype of IκBε-deficient mice. Analysis of this mutant nonetheless provides evidence for specific roles of IκBε in the regulation of cytokine synthesis and maybe Ig switching, which cannot be counterbalanced by other IκBs. These studies also illustrate the role of individual members of the IκB family in the tight control of NF-κB activity. Evaluation of the defects present in mice with a knockin of the *IκBε* gene at the *IκBα* locus or mice with simultaneous disruption of multiple IκBs should help to unravel the relative functions and biochemical differences betwen these molecules and to understand how NF-κB activity is controlled in vivo by individual IκBs.

Acknowledgments

S.M. thanks instructors and lecturers of the '95 Cold Spring Harbor Laboratory course on "The Molecular Embryology of the Mouse" for their wonderful training. We also thank Sharaghim Tajbashk for numerous gifts of plasmids, Didier Rocancourt for help in microinjection, Clémire Cimper for excellent tissue section assistance, Pierre Trotot for x-ray irradiation of the mice, Armelle Phalipon for initiation into mice intranasal inoculation with Shigella, Valérie Friedmacher for help in PhosphorImager analysis, and Robert Kelly for critical reading of the manuscript. We are also grateful to Nancy Rice, Rodrigo Bravo, and Robert Weil for providing us with sera, and to David Melton for his kind gift of HM1 ES cells.

References

1. Grilli, M., J. J. S. Chiu, and M. Lenardo. 1993. NF-κ-B and *rel*: participants in a multiform transcriptional regulatory system. *Int. Rev. Cytol. 143:1.*
2. May, M. J., and S. Ghosh. 1998. Signal transduction through NF-κB. *Immunol. Today 19:80.*
3. Baldwin, A. S. 1996. The NF-κB and IκB proteins: new discoveries and insights. *Annu. Rev. Immunol. 14:649.*
4. Attar, R. M., J. Caamano, D. Carrasco, V. Iotsova, H. Ishikawa, R. P. Ryseck, F. Weih, and R. Bravo. 1997. Genetic approaches to study *rel*/NF-κB/IκB function in mice. *Semin. Cancer Biol. 8:93.*
5. Gerondakis, S., R. Grumont, I. Rourke, and M. Grossmann. 1998. The regulation and roles of *rel*/NF-κB transcription factors during lymphocyte activation. *Curr. Opin. Immunol. 10:353.*
6. Ghosh, S., M. J. May, and E. B. Kopp. 1998. NF-κB and *rel* proteins: evolutionary conserved mediators of immune responses. *Annu. Rev. Immunol. 16:225.*
7. Sha, W. C. 1998. Regulation of immune responses by NF-κB/*rel* transcription factors. *J. Exp. Med. 187:143.*
8. Baeuerle, P. A., and T. Henkel. 1994. Function and activation of NF-κκB in the immune system. *Annu. Rev. Immunol. 12:141.*
9. Schmidt-Ullrich, R., S. Mémet, A. Lilienbaum, J. Feuillard, M. Raphael, and A. Israël. 1996. NF-κB activity in transgenic mice: developmental regulation and tissue specificity. *Development 122:2117.*
10. Whiteside, S. T., and A. Israel. 1997. IκB proteins: structure, function and regulation. *Semin. Cancer Biol. 8:75.*
11. Ghosh, S., and D. Baltimore. 1990. Activation in vitro of NF-κB by phosphorylation of its inhibitor IκB. *Nature 344:678.*
12. Zabel, U., and P. A. Baeuerle. 1990. Purified human IκB can rapidly dissociate the complex of the NF-κB transcription factor with its cognate DNA. *Cell 61: 255.*
13. Haskill, S., A. A. Beg, S. M. Tompkins, J. S. Morris, A. D. Yurochko, A. Sampson-Johannes, K. Mondal, P. Ralph, and A. S. Baldwin. 1991. Characterization of an immediate-early gene induced in adherent monocytes that encodes IκB-like activity. *Cell 65:1281.*
14. Thompson, J. E., R. J. Phillips, H. Erdjument-Bromage, P. Tempst, and S. Ghosh. 1995. IκBβ regulates the persistent response in a biphasic activation of NF-κB. *Cell 80:573.*
15. Whiteside, S. T., J. C. Epinat, N. R. Rice, and A. Israel. 1997. IκBε, a novel member of the IκB family, controls *relA* and c-*rel* NF-κB activity. *EMBO J. 16:1413.*
16. Li, Z., and G. J. Nabel. 1997. A new member of the IκB protein family, IκBε, inhibits *relA* (p65)-mediated NF-κB transcription. *Mol. Cell. Biol. 17:6184.*
17. Simeonidis, S., S. Liang, G. Y. Chen, and D. Thanos. 1997. Cloning and functional characterization of mouse IκBε. *Proc. Natl. Acad. Sci. USA 94:14372.*
18. Whiteside, S. T., M. K. Ernst, O. LeBail, C. Laurent-Winter, N. R. Rice, and A. Israel. 1995. N- and C-terminal sequences control degradation of MAD3/IκBα in response to inducers of NF-κB activity. *Mol. Cell. Biol. 15:5339.*
19. Arenzana Seisdedos, F., J. Thompson, M. S. Rodriguez, F. Bachelerie, D. Thomas, and R. T. Hay. 1995. Inducible nuclear expression of newly synthesized IκBα negatively regulates DNA-binding and transcriptional activities of NF-κB. *Mol. Cell. Biol. 15:2689.*
20. Arenzana Seisdedos, F., P. Turpin, M. Rodriguez, D. Thomas, R. T. Hay, J. L. Virelizier, and C. Dargemont. 1997. Nuclear localization of IκBα promotes active transport of NF-κB from the nucleus to the cytoplasm. *J. Cell Sci. 110:369.*
21. Suyang, H., R. Phillips, I. Douglas, and S. Ghosh. 1996. Role of unphosphorylated, newly synthesized IκBβ in persistent activation of NF-κB. *Mol. Cell. Biol. 16:5444.*
22. Beg, A. A., W. C. Sha, R. T. Bronson, S. Ghosh, and D. Baltimore. 1995. Embryonic lethality and liver degeneration in mice lacking the RelA component of NF-κB. *Nature 376:167.*
23. Klement, J. F., N. R. Rice, B. D. Car, S. J. Abbondanzo, G. D. Powers, H. Bhatt, C. H. Chen, C. A. Rosen, and C. L. Stewart. 1996. IκBα deficiency results in a sustained NF-κB response and severe widespread dermatitis in mice. *Mol. Cell. Biol. 16:2341.*
24. Cheng, J. D., R. P. Ryseck, R. M. Attar, D. Dambach, and R. Bravo. 1998. Functional redundancy of the nuclear factor κB inhibitors IκBα and IκBβ. *J. Exp. Med. 188:1055.*
25. Attar, R. M., H. Macdonald-Bravo, C. Raventos-Suarez, S. K. Durham, and R. Bravo. 1998. Expression of constitutively active IκBβ in T cells of transgenic mice: persistent NF-κB activity is required for T-cell immune responses. *Mol. Cell. Biol. 18:477.*
26. Boothby, M. R., A. L. Mora, D. C. Scherer, J. A. Brockman, and D. W. Ballard. 1997. Perturbation of the T lymphocyte lineage in transgenic mice expressing a constitutive repressor of nuclear factor NF-κB. *J. Exp. Med. 185:1897.*
27. Tybulewicz, V. L., C. E. Crawford, P. K. Jackson, R. T. Bronson, and R. C. Mulligan. 1991. Neonatal lethality and lymphopenia in mice with a homozygous disruption of the c-*abl* proto-oncogene. *Cell 65:1153.*

28. Laird, P. W., A. Zidjerveld, K. Linders, M. A. Rudnicki, R. Jaenisch, and A. Berns. 1991. Simplified mammalian DNA isolation procedure. *Nucleic Acids Res. 19:4293.*
29. Church, G. M., and W. Gilbert. 1984. Genomic sequencing. *Proc. Natl. Acad. Sci. USA 81:1991.*
30. Fiering, S., J. P. Northrop, G. P. Nolan, P. S. Mattila, G. R. Crabtree, and L. A. Herzenberg. 1990. Single cell assay of a transcription factor reveals a threshold in transcription activated by signals emanating from the T-cell antigen receptor. *Genes Dev. 4:1823.*
31. Phalipon, A., M. Kaufmann, P. Michetti, J.-M. Cavaillon, M. Huerre, P. Sansonetti, and J.-P. Kraehenbuhl. 1995. Monoclonal immunoglobulin A antibody directed against serotype-specific epitope of *Shigella flexneri* lipopolysaccharide protects against murine experimental shigellosis. *J. Exp. Med. 182:769.*
32. Gaillard, J. L., P. Berche, C. Fréhel, E. Gouin, and P. Cossart. 1991. Entry of *L. monocytogenes* into cells is mediated by internalin, a repeat protein reminiscent of surface antigen from Gram-positive cocci. *Cell 65:1127.*
33. Le Mouellic, H., Y. Lallemand, and P. Brulet. 1990. Targeted replacement of the homeobox gene Hox-3.1 by the *Escherichia coli* lacZ in mouse. *Proc. Natl. Acad. Sci. USA 87:4712.*
34. Jeannotte, L., J. C. Ruiz, and E. J. Robertson. 1991. Low level of Hox1.3 gene expression does not preclude the use of promoterless vectors to generate a targeted gene disruption. *Mol. Cell. Biol. 11:5578.*
35. Kim, D. G., H. M. Kang, S. K. Jang, and H.-S. Shin. 1992. Construction of a bifunctional mRNA in the mouse by using the internal ribosomal entry site of the encephalomyocarditis virus. *Mol. Cell. Biol. 12:3636.*
36. Mansour, S. L., K. R. Thomas, and M. R. Capecchi. 1988. Disruption of the proto-oncogene *int-2* in mouse embryo-derived stem cells: a general strategy for targeting mutations to non-selectable genes. *Nature 336:348.*
37. Yagi, T., Y. Ikawa, K. Yoshida, Y. Shigetani, N. Takeda, I. Mabuchi, T. Yamamoto, and S. Aizawa. 1990. Homologous recombination at c-*fyn* locus of mouse embryonic stem cells with use of diphtheria toxin A-fragment gene in negative selection. *Proc. Natl. Acad. Sci. USA 87:9918.*
38. Nolan, G. P., S. Fiering, J. F. Nicolas, and L. A. Herzenberg. 1988. Fluorescence-activated cell analysis and sorting of viable mammalian cells based on β-D-galactosidase activity after transduction of *Escherichia coli lacZ. Proc. Natl. Acad. Sci. USA 85:2603.*
39. Hardy, R. R., C. E. Carmack, S. A. Shinton, J. D. Kemp, and K. Hayakawa. 1991. Resolution and characterization of pro-B and pre-pro-B cell stages in normal mouse bone marrow. *J. Exp. Med. 173:1213.*
40. Ziegler-Heitbrock, H. W. L. 1989. The biology of the monocyte system. *Eur. J. Cell Biol. 49:1.*
41. Eckmann, L., M. F. Kagnoff, and J. Fierer. 1993. Epithelial cells secrete the chemokine interleukin-8 in response to bacterial entry. *Infect. Immun. 61:4569.*
42. Jung, H. C., L. Eckmann, S.-K. Yang, A. Panja, J. Fierer, E. Morzycka-Wroblewska, and M. F. Kagnoff. 1995. A distinct array of proinflammatory cytokines is expressed in human colon epithelial cells in response to bacterial invasion. *J. Clin. Invest. 95:55.*
43. Kayal, S., A. Lilienbaum, C. Poyart, S. Mémet, A. Israël, and P. Berche. 1999. Listeriolysin O-dependent activation of endothelial cells during infection with *Listeria monocytogenes*: activation of NF-κB and up-regulation of adhesion molecules and chemokines. *Mol. Microbiol. 31:1709.*
44. Beg, A. A., W. C. Sha, R. T. Bronson, and D. Baltimore. 1995. Constitutive NF-κB activation, enhanced granulopoiesis, and neonatal lethality in IκBα-deficient mice. *Genes Dev. 9:2736.*
45. Fiering, S. N., M. Roederer, G. P. Nolan, D. R. Micklem, D. R. Parks, and L. A. Herzenberg. 1991. Improved FACS-Gal: flow cytometric analysis and sorting of viable eukaryotic cells expressing reporter gene constructs. *Cytometry 12:291.*
46. Brown, K., S. Park, T. Kanno, G. Franzoso, and U. Siebenlist. 1993. Mutual regulation of the transcriptional activator NF-κB and its inhibitor, IκBα. *Proc. Natl. Acad. Sci. USA 90:2532.*
47. LeBail, O., R. Schmidt Ullrich, and A. Israel. 1993. Promoter analysis of the gene encoding the IκBα/MAD3 inhibitor of NF-κB: positive regulation by members of the *rel*/NF-κB family. *EMBO J. 12:5043.*
48. Rice, N. R., and M. K. Ernst. 1993. In vivo control of NF-κB activation by IκBα. *EMBO J. 12:4685.*
49. Scott, M. L., T. Fujita, H. C. Liou, G. P. Nolan, and D. Baltimore. 1993. The p65-subunit of NF-κB regulates IκB by 2 distinct mechanisms. *Genes Dev. 7:1266.*
50. Sun, S. C., P. A. Ganchi, D. W. Ballard, and W. C. Greene. 1993. NF-κB controls expression of inhibitor IκBα: evidence for an inducible autoregulatory pathway. *Science 259:1912.*
51. Godfrey, D. I., and A. Zlotnik. 1993. Control points in early T-cell development. *Immunol. Today 14:547.*
52. Willerford, D. M., J. Chen, J. A. Ferry, L. Davidson, A. Ma, and F. W. Alt. 1995. Interleukin-2 receptor α chain regulates the size and content of the peripheral lymphoid compartment. *Immunity 3:521.*
53. Kontgen, F., R. J. Grumont, A. Strasser, D. Metcalf, R. L. Li, D. Tarlinton, and S. Gerondakis. 1995. Mice lacking the c-*rel* proto-oncogene exhibit defects in lymphocyte proliferation, humoral immunity, and interleukin-2 expression. *Genes Dev. 9:1965.*
54. Weih, F., D. Carrasco, S. K. Durham, D. S. Barton, C. A. Rizzo, R. P. Ryseck, S. A. Lira, and R. Bravo. 1995. Multiorgan inflammation and hematopoietic abnormalities in mice with a targeted disruption of RelB, a member of the NF-κB/Rel family. *Cell 80:331.*
55. Sha, W. C., H. C. Liou, E. I. Tuomanen, and D. Baltimore. 1995. Targeted disruption of the p50 subunit of NF-κB leads to multifocal defects in immune responses. *Cell 80:321.*
56. Doi, T. S., T. Takahashi, O. Taguchi, T. Azuma, and Y. Obata. 1997. NF-κB *relA*-deficient lymphocytes: normal development of T cells and B cells, impaired production of IgA and IgG1 and reduced proliferative responses. *J. Exp. Med. 185:953.*
57. Franzoso, G., L. Carlson, L. P. Xing, L. Poljak, E. W. Shores, K. D. Brown, A. Leonardi, T. Tran, B. F. Boyce, and U. Siebenlist. 1997. Requirement for NF-κB in osteoclast and B-cell development. *Genes Dev. 11:3482.*
58. Caamano, J. H., C. A. Rizzo, S. K. Durham, D. S. Barton, C. Raventos-Suarez, C. M. Snapper, and R. Bravo. 1998. Nuclear factor (NF)-κB2 (p100/p52) is required for normal splenic microarchitecture and B cell-mediated immune responses. *J. Exp. Med. 187:185.*
59. Franzoso, G., L. Carlson, L. Poljak, E. W. Shores, S. Epstein, A. Leonardi, A. Grinberg, T. Tran, T. Schartonkersten, M. Anver, P. Love, K. Brown, and U. Siebenlist. 1998. Mice deficient in nuclear factor (NF)-κB/p52 present with defects in humoral responses, germinal center reactions, and splenic microarchitecture. *J. Exp. Med. 187:147.*
60. Cogné, M., R. Lansdorf, A. Bottaro, J. Zhang, J. Gorman, F. Young, H.-L. Cheng, and F. W. Alt. 1994. A class switch control region at the 3′ end of the immunoglobulin heavy chain locus. *Cell 77:737.*
61. Michaelson, J. S., M. Singh, C. M. Snapper, W. C. Sha, D. Baltimore, and B. K. Birshtein. 1996. Regulation of 3′ IgH enhancers by a common set of factors including κB-binding proteins. *J. Immunol. 156:2828.*
62. Lin, S. C., and J. Stavnezer. 1996. Activation of NF-κB/Rel by CD40 engagement induces the mouse germ line immunoglobulin Cγ1 promoter. *Mol. Cell. Biol. 16:4591.*
63. Iciek, L. A., S. A. Delphin, and J. Stavnezer. 1997. CD40 cross-linking induces Ig-ε germline transcripts in B cells via activation of NF-κB: synergy with IL-4 induction. *J. Immunol. 158:4769.*
64. Weih, F., G. Warr, H. Yang, and R. Bravo. 1997. Multifocal defects in immune responses in *relB*-deficient mice. *J. Immunol. 158:5211.*
65. Hiscott, J., J. Marois, J. Garoufalis, M. D'Addario, A. Roulston, I. Kwan, N. Pepin, J. Lacoste, H. Nguyen, G. Bensi, and M. Fenton. 1993. Characterization of a functional NF-κB site in the human interleukin 1β promoter: evidence for a positive autoregulatory loop. *Mol. Cell. Biol. 13:6231.*
66. Cogswell, J. P., M. M. Godlevski, G. B. Wisely, W. C. Clay, L. M. Leesnitzer, J. P. Ways, and J. G. Gray. 1994. NF-κB regulates IL-1β transcription through a consensus NF-κB binding site and a nonconsensus CRE-like site. *J. Immunol. 153:712.*
67. Parry, G. C. N., and N. Mackman. 1994. A set of inducible genes expressed by activated human monocytic and endothelial cells contain κB-like sites that specifically bind c-Rel-p65 heterodimers. *J. Biol. Chem. 269:20823.*
68. Vincent, S., L. Marty, and P. Fort. 1993. S26 ribosomal protein RNA: an invariant control for gene regulation experiments in eucaryotic cells and tissues. *Nucleic Acids Res. 21:1498.*